CT&F Ciencia, Tecnología y Futuro
ISSN: 0122-5383
ctyf@ecopetrol.com.co
ECOPETROL S.A.
Colombia

Escobar, Freddy- Humberto; Sánchez, Jairo Andrés; Cantillo, José Humberto
RATE TRANSIENT ANALYSIS FOR HOMOGENEOUS AND HETEROGENEOUS GAS RESERVOIRS USING THE TDS TECHNIQUE
CT&F Ciencia, Tecnología y Futuro, vol. 3, núm. 4, diciembre, 2008, pp. 45-59
ECOPETROL S.A.
Bucaramanga, Colombia

CT&F
Ciencia, Tecnología y Futuro

RATE TRANSIENT ANALYSIS FOR HOMOGENEOUS AND HETEROGENEOUS GAS RESERVOIRS USING THE TDS TECHNIQUE

Freddy- Humberto Escobar[1]*, Jairo Andrés Sánchez[2] and José Humberto Cantillo[3]

[1,2] Universidad Surcolombiana, Programa de Ingeniería de Petróleos, Grupo de Investigación en Pruebas de Pozos, Neiva, Huila, Colombia
[3] Ecopetrol S.A.- Instituto Colombiano del Petróleo, A.A. 4185 Bucaramanga, Santander, Colombia

e-mail: fescobar@usco.edu.co

(Received May 30, 2008; Accepted Dec. 5, 2008)

In this study pressure test analysis in wells flowing under constant wellbore flowing pressure for homogeneous and naturally fractured gas reservoir using the TDS technique is introduced. Although, constant rate production is assumed in the development of the conventional well test analysis methods, constant pressure production conditions are sometimes used in the oil and gas industry. The constant pressure technique or rate transient analysis is more popular reckoned as “decline curve analysis” under which rate is allows to decline instead of wellbore pressure.

The TDS technique, everyday more used even in the most recognized software packages although without using its trade brand name, uses the log-log plot to analyze pressure and pressure derivative test data to identify unique features from which exact analytical expression are derived to easily estimate reservoir and well parameters. For this case, the “fingerprint” characteristics from the log-log plot of the reciprocal rate and reciprocal rate derivative were employed to obtain the analytical expressions used for the interpretation analysis. Many simulation experiments demonstrate the accuracy of the new method. Synthetic examples are shown to verify the effectiveness of the proposed methodology.

Keywords: *radial flow, closed system, pseudosteady state, interporosity flow parameter, dimensionless storage coefficient, fracture dominated period, transition period.*

***** *To whom correspondence may be addressed*

En este estudio se introduce el análisis de pruebas de presión en pozos de gas que fluyen a presión de fondo constante en formaciones homogéneas y naturalmente fracturadas usando la técnica TDS. Aunque normalmente se considera la producción de un pozo a caudal constante en el desarrollo de los métodos convencionales de interpretación de pruebas de pozos, el caso de producción de un pozo a condiciones de presión constante se usa en algunas ocasiones en la industria de los hidrocarburos. La técnica de presión constante o análisis de transientes de caudal se conoce más popularmente como "análisis de curvas de declinación" en la cual se permite que la rata de flujo decline en vez de hacerlo la presión del pozo.

La técnica TDS se vuelve más popular cada día incluso en la mayoría de los programas comerciales que aunque sin usar su nombre de pila, usan el gráfico log-log para analizar datos de presión y la derivada de presión para identificar características únicas de las cuales se derivan relaciones analíticas exactas para estimar fácilmente los parámetros del yacimiento y el pozo. Para este caso "las huellas digitales" características procedentes del gráfico log-log del recíproco del caudal y la derivada del recíproco del caudal se emplearon para obtener expresiones analíticas que se usan para propósitos de interpretación. Se usaron muchas corridas de simulación para demostrar la exactitud del nuevo método. Se muestran ejemplos sintéticos para verificar la efectividad de la metodología propuesta.

Palabras Clave: *flujo radial, sistema cerrado, estado pseudoestable, parámetro de flujo interporoso, coeficiente de almacenamiento adimensional, periodo dominado por las fracturas, periodo de transición.*

NOMENCLATURE

A	Drainage area, ft^2
B	Volumetric factor, rb/MSCF
C	Wellbore storage coefficient, bbl/psi
c_t	Total compressibility, 1/psi
D	Turbulent flow factor, Mscf/D
h	Formation thickness, ft
I_0, I_1	Bessel function
K_0,K_1	Bessel function
k_f	Fracture network permeability, md
$m(P)$	Pseudopropressure function, psi^2/cp
P	Pressure, psi
P_D	Dimensionless pressure
P_{wf}	Well-flowing pressure, psi
q	Rate, MSCF
$1/q$	Reciprocal of the flow rate, D/Mscf
r	Radius, ft
r_e	External reservoir radius, ft
r_w	Radio del pozo, ft
r_{weff}	Effective wellbore radius, $r_w e^{-s}$, ft
s'	Apparent skin factor
s_t	Total skin factor
t	Time, hr
t_D*P_D'	Dimensionless pressure derivative
$t*(1/q)'$	Reciprocal rate derivative, D/Mscf
$t_D*(1/q_D)'$	Dimensionless reciprocal rate derivative
t_{pss}	Time to initiate pseudosteady state, hr
u	Argument for a Bessel function

GREEK SYMBOLS

Δ	Change, drop
ϕ	Porosity, fraction
λ	Interporosity flow parameter
μ	Viscosity, cp
ω	Dimensionless storativity coefficient

SUBINDEXES

$b2$	Beginning of the second radial flow
D	Dimensionless
$e1$	Ending of the first radial flow
eff	Effective
f	Fractures
i	Initial
inf	Inflection point. Transition period where $(1/q)$ curve is horizontal
N	A point during the early unit-slope line
m	Matrix
max	Maximum point on the reciprocal rate derivative curve
min	Mainimum point on the reciprocal rate derivative curve
r	Radial flow
$r1$	First radial flow
$r2$	Second radial flow
rdi	Intercept of the reciprocal rate curve with its derivative
rpi	Intercept radial-pseudosteady
sr	Start of radial flow
t	Total
us	Any convenient point on the unit-slope line (transition period)
us,i	Interception of the radial and unit-slope (transition period) lines
us,h	Intercept of the late pseudosteady state and the horizontal reciprocal rate line during the transition period
w	Well

INTRODUCTION

Normally, well test interpretation methods assume well production at a given constant rate. However, several common reservoir production conditions result in flow at a constant pressure, instead. Such is the case in wells producing from low permeability formations which often become necessary the production at a constant wellbore flowing pressure.

A gas or oil well producing at constant bottomhole pressure behaves analogously to that of a well operating at constant flow rate. In a constant pressure flow testing, the well produces at a constant sandface pressure and flow rate is recorded with time. Since rate solutions are found on basic flow principles, initially solved by Van Everdingen and Hurst (1949), flow rate data can be used for reservoir characterization. Therefore, this technique becomes in an alternative to conventional constant flow rate well testing techniques.

Several rate analysis methods are presented in the literature. The most popular method is the decline curve analysis presented by Fetkovich (1980) which is only applicable to circular homogeneous reservoirs. This technique assumes circular homogeneous reservoir and is not applicable to heterogeneous systems. The main drawback of type-curve matching, used by Fetkovich, is basically the involvement of a trial and error procedure which frequently provides multiple solutions. Therefore, a procedure used by Tiab (1995), TDS technique, avoids using type-curve matching since particular solutions are obtained from the pressure and pressure derivative plot providing a very practical methodology for interpretation of well tests. The application of the TDS technique to constant bottomhole pressure tests is not new. It was first introduced by Arab (2003) for the case of oil in homogeneous and heterogeneous reservoirs. Then, in this work, we extend Arab's work for gas well test interpretation.

MATHEMATICAL MODELING

Homogeneous reservoirs

The dimensionless quantities are defined as follows in *Equations 1, 2.a, 2.b,* and *4:*

$$1/q_D = \frac{khm\,\Delta(P)}{1422{,}52Tq} \tag{1}$$

$$t_D = \frac{0{,}0002637kt}{\phi\mu c_t r_w^2} \tag{2.a}$$

$$t_{DA} = \frac{0{,}0002637kt}{\phi\mu c_t A} \tag{2.b}$$

$$C_D = \frac{0{,}8935C}{\phi c_t h r_w^2} \tag{3}$$

The solutions to the flow equation under constant well pressure for an infinite reservoir including wellbore damage, Van Everdingen and Hurst (1949), and bounded reservoir, DPrat, Cinco-Ley, and Ramey (1981), respectively, are *Equations 4.a* and *4.b:*

$$\bar{q}_D = \frac{K_1(\sqrt{u}\,)}{\sqrt{u}\left[K_0(\sqrt{u}) + s\sqrt{u}K_1(\sqrt{u})\right]} \tag{4.a}$$

$$\bar{q}_D = \frac{I_1(r_{eD}\sqrt{u})K_1(\sqrt{u}) - K_1(r_{eD}\sqrt{u})I_1(\sqrt{u})}{\sqrt{u}\left[I_0(\sqrt{u})K_1(r_{eD}\sqrt{u}) + K_0(\sqrt{u})I_1(r_{eD}\sqrt{u})\right]} \tag{4.b}$$

By analogy with transient pressure analysis, during the early time period of the reciprocal rate a unit-slope line is identified. The equation of this line is *Equation 5:*

$$1/q_D = \frac{t_D}{C_D} \tag{5}$$

The relationship t_D/C_D is obtained from the combination of *Equations 2.a* and *3:*

$$\frac{t_D}{C_D} = 2{,}95\times10^{-4}\frac{kht}{\mu C} \tag{6}$$

Substituting *Equations 1* and *6* into *Equation 5* will result an expression for the wellbore storage coefficient:

$$C = 0{,}4196\frac{Tqt_N}{\mu\,\Delta m(P)_N} \tag{7}$$

The reciprocal rate derivative also has a unit-slope line at early times. Its equation is *Equation 8:*

$$\frac{t_D}{C_D}(1/q_D)' = \frac{t_D}{C_D} \tag{8}$$

The derivative of the reciprocal flow rate is given by:

$$(1/q_D)' = 2{,}6658\frac{h\phi\mu c_t r_w^2\Delta m(P)}{T}(1/q)' \tag{9}$$

The left-hand side of *Equation 8* can be combined by replacing *Equations 6* and *9* and after multiplying and diving by 0,8935 (to replace by C_D) and taking C_D as 1, finally results in *Equation 10:*

$$\frac{t_D}{C_D}\left(1/q_D\right)' = 7{,}0266\times10^{-4}\,\frac{kh\Delta m(P)}{T}\left[t*\left(1/q\right)'\right] \quad (10)$$

Also, during the early time period the reciprocal rate derivative has a unit-slope line is identified, which allows to obtain *Equation 11:*

$$C = 0{,}4198\,\frac{T}{\mu\,\Delta m(P)}\left[\frac{t}{t\times\left(1/q\right)'}\right]_N \quad (11)$$

As shown in Figure 1, the horizontal line of the reciprocal pressure derivative during infinite- acting behavior is described by *Equation 12:*

$$\left[\frac{t_D}{C_D}\left(1/q_D\right)'\right]_r = 0{,}5 \quad (12)$$

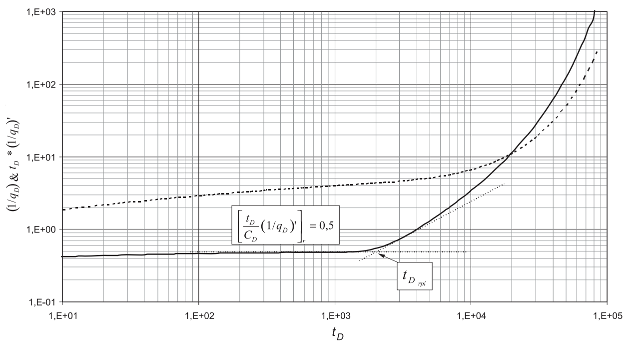

Figure 1. Log-Log plot of dimensionless reciprocal rate and reciprocal rate derivative for a homogeneous bounded reservoir

Combining *Equations 10* and *12* results in an expression to estimate formation permeability,

$$k = 711{,}5817\,\frac{T}{h\Delta m(P)\left[t\times\left(1/q\right)'\right]_r} \quad (13)$$

According to Tiab (1995) the starting time of the infinite-acting line of the reciprocal rate derivative can be approximated by *Equation 14:*

$$\left(\frac{t_D}{C_D}\right)_{sr} = 10\log\left(C_D e^{2s}\right)^{10} \quad (14)$$

Plugging *Equation 6* and *3* into *Equation 13* provides an equation to estimate the starting time of the radial flow regime:

$$t_{sr} = 147218{,}4684\,\frac{\mu C}{kh}\left[\ln\left(\frac{0{,}8935C}{\phi c_t h r_w^{\,2}}\right) + 2s\right] \quad (15)$$

According to Vongvuthipornchai and Raghavan (1988), the start of the radial flow line is represented by *Equation 16:*

$$\left(\frac{t_D}{C_D}\right)_{sr} = \frac{1}{\alpha}\left[\ln(C_D e^{2s}) + \ln\left(\frac{t_D}{C_D}\right)_{sr}\right] \quad (16)$$

Being α a tolerance factor which may be substituted by 0,05 giving results within 8% of accuracy. Replacing *Equation 3* into *Equation 16,* it yields in *Equation 17:*

$$C = 0{,}056\phi c_t h r_w^2\left[\frac{t_{Dsr}}{2s + \ln\left(t_{Dsr}\right)}\right] \quad (17)$$

t_{Dsr} is found from *Equation 2.a* for $t = t_{Dsr}$. From the intercept between the early unit-slope and radial lines results in an expression useful to verify permeability, *Equation 18:*

$$t_i = 1695\,\frac{\mu C}{kh} \quad (18)$$

Tiab (1995) correlated permeability, skin factor and wellbore storage coefficient with the maximum pressure derivative point during the early transition period. By analogy, from those correlations we obtain *Equations 19, 20,21, 22* and *23:*

$$k = 597{,}7286\,\frac{T}{h\Delta m(P)} / 0{,}1511\,\frac{Tt_x}{\mu C\Delta m(P)} - \left[t\times\left(1/q\right)'\right]_x \quad (19)$$

$$s' = 0{,}1703\left(\frac{t_x}{t_i}\right)^{1{,}24} - 0{,}5\ln\left(\frac{0{,}8935C}{\phi c_t h r_w^{\,2}}\right) \quad (20)$$

$$s' = 0{,}9184\left\{\frac{\left[t\times(1/'q)\right]_x}{\left[t\times(1/'q)\right]_r}\right\}^{1,1} - 0{,}5\ln\left(\frac{0{,}8935C}{\phi c_t h r_w^2}\right) \quad (21)$$

$$C = \frac{0{,}1511Tt_x}{\left\{\left[t\times(1/q)'\right]_x + 0{,}84\left[t\times(1/q)'\right]_r\right\}\mu\Delta m(P)} \quad (22)$$

$$k = 9416{,}1958\frac{\mu C}{ht_x}\left\{0{,}5\frac{\left[t\times(1/'q)\right]_x}{\left[t\times(1/'q)\right]_r} + 0{,}42\right\} \quad (23)$$

For constant pressure production during radial, $t_D >$ 8000, the reciprocal rate behavior including skin factor obeys the following behavior, Equation 24:

$$1/q_{Dr} = 0{,}5\left[\ln(t_D) + 0{,}80907 + 2s'\right] \quad (24)$$

Dividing *Equation 24* by *Equation 12,* plugging the dimensionless quantities and, then, solving for the apparent skin factor results *Equation 25:*

$$s' = 0{,}5\left\{\frac{(1/q)_r}{\left[t\times(1/'q)\right]_r} - \ln\left(\frac{kt_r}{\phi\mu c_t r_w^2}\right) + 7{,}43\right\} \quad (25)$$

Arab (2003) found that the pseudosteady state develops when t_{DA} = 0,0054 (t_{DApss} = 0,0054). Replacing this into *Equation 2.b* and knowing that for circular systems $A = \pi r_e^2$, the external radius can be found as *Equation 26:*

$$r_e^2 = \left(\frac{0{,}0015kt}{\phi\mu c_t}\right)^{1/2} \quad (26)$$

As seen in Figure 1, the intercept formed between radial and pseudosteady state lines of the dimensionless reciprocal derivative is defined as, Arab (2003):

$$t_{D_{rpi}} = \frac{1}{2}r_{eD}^2\left[\ln(r_{eD}) - 0{,}75\right] \quad (27)$$

Which numerical solution, Arab (2003), leads to *Equation 28:*

$$r_{eD} = 1{,}0292\,t_{D_{rpi}}^{0,4627} \quad (28)$$

Defining the dimensionless external radius by *Equation 29:*

$$r_{eD} = \frac{r_e}{r_w e^{-s}} = \frac{r_e}{r_{weff}} \quad (29)$$

After replacing *Equation 2.a* and *29* into *Equation 28* yields in *Equation 30:*

$$r_e = 22{,}727\times10^{-3}\,r_{weff}\left(\frac{k}{\phi\mu\, c r_{tweff}^2}\right)^{0,4627} t_{rpi}^{\;0,4627} \quad (30)$$

Heterogeneous reservoirs

Transition period occurs during radial flow regime

Redefining *Equation 2.b:*

$$t_D = \frac{0{,}0002637k_f t}{(\phi c)_{f+m}\mu r_w^2} \quad (31)$$

From here on, k in *Equation 1* and *3* is replaced by k_f representing the network fracture permeability. The naturally fractured reservoir parameters, Warren and Root (1963), are given by *Equation 32:*

$$\omega = \frac{\phi_f c_f}{\phi_m c_m + \phi_f c_f} \quad (32)$$

$$\lambda\alpha \ \frac{k_m}{k_f} \quad (33)$$

Here α means "proportional" and is not the same as in *Equation 16.* Define the reservoir storativity as *Equation 34:*

$$S_t = \phi c_t h = (\phi c)_{m+f}h \quad (34)$$

The solution of the diffusivity equation for an infinite and bounded heterogeneous reservoir, respectively, was presented by DPrat, Cinco-Ley, and Ramey (1981):

$$\bar{q}_D = \frac{\sqrt{uf(u)}K_1\left(\sqrt{uf(u)}\right)}{u\left[K_0\left(\sqrt{uf(u)}\right)+s\sqrt{uf(u)}K_1\left(\sqrt{uf(u)}\right)\right]} \qquad (35.a)$$

$$\bar{q}_D=\sqrt{uf(u)}\,\frac{\left[I_1\left(\sqrt{uf(u)}r_{eD}\right)K_1\left(\sqrt{uf(u)}\right)-K_1\left(\sqrt{uf(u)}r_{eD}\right)I_1\left(\sqrt{uf(u)}\right)\right]}{u\left\{K_1\left(\sqrt{uf(u)}r_{eD}\right)I_0\left(\sqrt{uf(u)}\right)+I_1\left(\sqrt{uf(u)}r_{eD}\right)K_0\left(\sqrt{uf(u)}\right)\right.} \qquad (35.b)$$

$$\overline{\left.\sqrt{uf(u)}\,u\left[K_1\left(\sqrt{uf(u)}r_{eD}\right)I_1\left(\sqrt{uf(u)}\right)-I_1\left(\sqrt{uf(u)}\right)K_1\left(\sqrt{uf(u)}r_{eD}\right)\right]\right\}}$$

where variable *f (u)* is defined by *Equation 35.c :*

$$f(u)=\frac{\omega\left(1-\omega\right)u+\lambda}{\left(1-\omega\right)u+\lambda} \qquad (35.c)$$

Arab (2003) found that the solution for the pressure and reciprocal rate behaves similarly, Figure 3, then, the reciprocal rate solution and its derivative for a naturally fractured reservoir obey the following expressions, *Equations 35.d* and *35.e :*

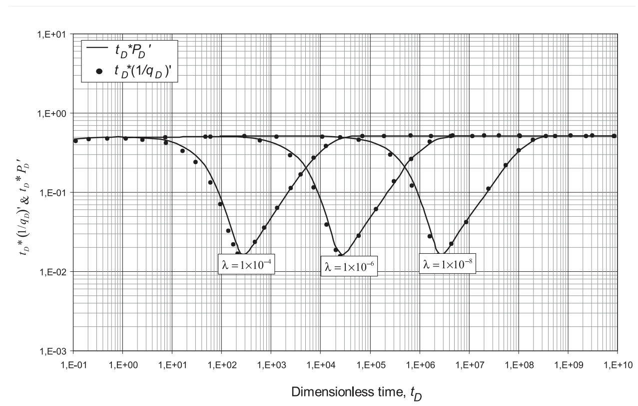

Figure 3. Comparison between the constant flow rate solution and constant pressure production solution (ω = 0,005), after Arab (2003)

$$1/q_D=\frac{1}{2}\left[\ln\left(t_D\right)+0{,}80907+E_i\left(-\frac{\lambda t_D}{\omega(1-\omega)}\right)-E_i\left(-\frac{\lambda t_D}{(1-\omega)}\right)\right] \qquad (35.d)$$

$$t_D\times(1/q_D)'=\frac{1}{2}\left[1-\exp\left(-\frac{\lambda t_D}{\omega\left(1-\omega\right)}\right)+\exp\left(-\frac{\lambda t_D}{\left(1-\omega\right)}\right)\right] \qquad (35.e)$$

In Figure 2, it is observed that the radial flow period has two segments. The first corresponds to fluid depletion inside the fracture network and the second one is the answer of a homogeneous system. Then, as for the homogeneous case, the pressure derivative during this period is represented by an expression similar to *Equation 12:*

$$t_D\times(1/q_D)'=0{,}5 \qquad (36)$$

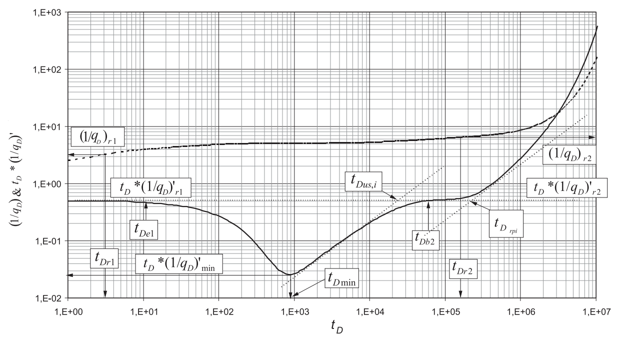

Figure 2. Log-log plot of reciprocal rate and reciprocal rate derivative for a naturally fractured bounded reservoir with λ = 0,0005, ω = 0,01 and r_{eD} = 1000

Again, after plugging the dimensionless quantities as for the homogeneous case, taking care that the dimensionless time is now represented by *Equation 31*, will result *Equation 37:*

$$k_f = 711{,}2664\,\frac{T}{h\Delta m(P)\left[t\times\left(1/q\right)'\right]_{r1\,\mathrm{or}\,r2}} \qquad (37)$$

Similarly to the procedure achieved by Engler and Tiab (1996), a log-log plot $[t_D*(1/q_D)']_{min}$ vs. $(\lambda t_D)_{min}$ results in a unit-slope straight line which equation is given by *Equation 38:*

$$\ln\left[t_D\times\left(1/q_D\right)'\right]_{\min}=\ln\left[\lambda t_{D\min}\right]+\ln(0{,}63) \qquad (38)$$

After replacing the dimensionless expressions and solving for the interporosity flow parameter,

$$\lambda = 4{,}2314\,\frac{S_t\mu r_w^{\,2}\Delta m(P)}{T}\left[\frac{t\times\left(1/q\right)'}{t}\right]_{\min} \qquad (39)$$

The transient behavior of a double porosity formation during the fracture-dominated period is given by, Engler and Tiab (1996), *Equation 40:*

$$(1/q_D)_{r1} = 0{,}5\left[\ln(t_{Dr1}) + 0{,}80907 + \ln\left(\frac{1}{\omega}\right)\right] + s \qquad (40)$$

After dividing the above relationship by *Equation 36*, replacing the dimensionless parameters and solving for the apparent skin factor results *Equation 41.a:*

$$s' = 0{,}5\left\{\left[\frac{(1/q_D)}{t\times(1/q)'}\right]_{r1} - \ln\left(\frac{k_f t_{r1}}{(\phi c)_{m+f}\,\mu\, r_w^2}\frac{1}{\omega}\right) + 7{,}43\right\} \qquad (41.a)$$

Once the transition period vanishes, the system behaves as homogeneous, then ω = 1, and *Equation 41.a* becomes *Equation 41. b:*

$$s' = 0{,}5\left\{\left[\frac{(1/q_D)}{t\times(1/q)'}\right]_{r2} - \ln\left(\frac{k_f t_{r2}}{(\phi c)_{m+f}\,\mu r_w^2}\right) + 7{,}43\right\} \qquad (41.b)$$

Referring to Figure 2, as expressed by Engler and Tiab (1996), the minimum point coordinates of the reciprocal rate derivative are *Equations 42.a* and *42.b:*

$$(t_D)_{\min} = \frac{\omega}{\lambda}\ln\left(\frac{1}{\omega}\right) \qquad (42.a)$$

$$\left[t_D\times(1/q_D)'\right]_{\min} = \frac{1}{2}\left[1 - \omega^{\left(\frac{\omega}{1-\omega}\right)} + \omega^{\left(\frac{1}{1-\omega}\right)}\right] \qquad (42.b)$$

Engler and Tiab (1996) divided *Equation 42.b* by *Equation 36* and plotted the ratio of the minimum and the radial pressure derivatives against the dimensionless storativity ratio. By the analogy obtained from Figure 3, the expression their expression is formulated as Equation 43:

$$\omega = 0{,}15866\frac{\left[t_D\times(1/q_D)'\right]_{\min}}{\left[t_D\times(1/q_D)'\right]_r} + 0{,}54653\left\{\frac{\left[t_D\times(1/q_D)'\right]_{\min}}{\left[t_D\times(1/q_D)'\right]_r}\right\}^2 \qquad (43)$$

Following the work done by Engler and Tiab (1996) and later by Arab (2003), the following relationship is presented in *Equation 44:*

$$\frac{50t_{e1}}{\omega(1-\omega)} = \frac{t_{e2}}{5(1-\omega)} = \frac{t_{\min}}{\omega\ln(1/\omega)} \qquad (44)$$

Arab (2003) defined the unit-slope line during the transition period as *Equation 45:*

$$\ln\left[t_D\times(1/q_D)'\right]_{us} = \ln\left(\frac{\lambda t_D}{2}\right) \qquad (45)$$

From the intercept point formed by the radial flow and the unit-slope lines will result *Equation 46:*

$$t_{D_{us,i}} = \frac{1}{\lambda} \qquad (46)$$

Plugging *Equation 31* into the above expression yields in *Equation 47:*

$$\lambda = \frac{(\phi c)_{f+m}\,\mu\, r_w^2}{0{,}0002637 k_f t_{us,i}} \qquad (47)$$

Equation 45 can be written as *Equation 48:*

$$t_{D_{us,i}} = -\frac{2}{\lambda}\left[\ln\left(\frac{\sqrt{\lambda}}{2}\right) + 0{,}57721 - s\right] \qquad (48)$$

Also, replacing *Equation 31* in the former equation results *Equation 49.a:*

$$t_{us,i} = -\frac{(\phi c)_t\,\mu\, r_w^2}{0{,}0001318 k_f}\frac{1}{\lambda}\left[\ln\left(\frac{\sqrt{\lambda}}{2}\right) + 0{,}57721 - s\right] \qquad (49.a)$$

Equation 49.a is useful to verify the value of λ. Other equations used in the conventional method to find the naturally fractured reservoir parameters can be applied for the case of constant pressure case, i.e., the equation presented by Tiab and Escobar (2003).

$$\lambda = \frac{3792\left(\phi c_t\right)_{m+f}\,\mu\, r_w^2}{k_f\, t_{\inf}}\left[\omega \ln\left(\frac{1}{\omega}\right)\right] \tag{49.b}$$

Being tinf the inflection point found during the transition period on the semilog plot. This time value also corresponds to the minimum point of time, t_{min}, found on the pressure derivative plot. Therefore, *Equation 49.b* forms part of the TDS technique.

Transition period occurs during late-pseudosteady state flow regime

The dimensionless time based upon area for a heterogeneous formation can be expressed by *Equation 50:*

$$t_{DA} = \frac{t_D}{\pi\, r_{eD}^{\ 2}\,\omega} \tag{50}$$

As seen in Figure 4, Arab (2003) found that the pseudosteady state develops when t_{DApss} = 0,00554. Assuming that the skin factor is zero in *Equation 29*, then from *Equation 50* will result *Equation 51:*

$$\omega = 4{,}7599\times 10^{-3}\,\frac{k_f\, t_{pss}}{\pi\, r_e^{\ 2}\left(\phi c\right)_t \mu} \tag{51}$$

Arab (2003) found the following correlation using the maximum point on the pressure derivative curve when the transition period initiates. *Equation 52:*

$$\lambda = \exp\left[-\ln\left(60{,}36\times 10^{-4}\frac{k_f\, h\left(P_i - P_{wf}\right)}{B\mu}\left[t^*(1/q)'\right]_{\max}\left(\frac{r_e}{r_w e^{-s}}\right)^{2{,}4815}\right)/1{,}2017\right] \tag{52}$$

Figures 4 and 5 show the different features found on the plot of reciprocal rate and reciprocal rate derivative. The unit-slope line of the transition period during the pseudosteady state, Figures 4 and 5, is governed by, Arab (2003):

$$\ln\left[t_D \times \left(1/q_D\right)'\right] = \ln\left(\frac{6{,}79}{\pi\, r_{eD}^{\ 2}}\, t_{D_{Uus}}\right) \tag{53}$$

Replacing the dimensionless equations an expression to obtain drainage area from any arbitrary point during the pseudosteady-state line (transition period) is obtained *Equation 54:*

$$r_e = \sqrt{0{,}8107\,\frac{T}{\left(\phi c\right)_t \mu\, h \Delta m(P)}\,\frac{t_{us}}{\left[t\times\left(1/'q\right)\right]_{us}}} \tag{54}$$

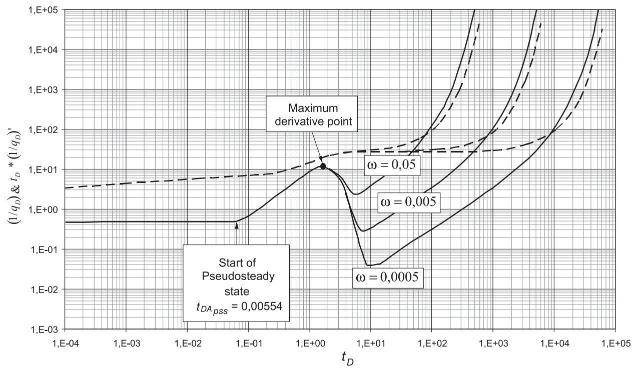

Figure 4. Effect of storage coefficient on the reciprocal rate response in naturally fractured reservoir, bounded reservoir, after Arab (2003)

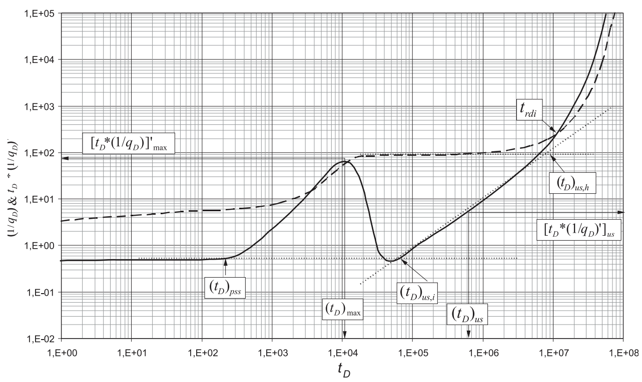

Figure 5. Characteristic points and lines in the answer of the reciprocal rate and its derivative for naturally fractured bounded reservoirs $\lambda = 1\text{x}10^{-7}$, ω = 0,0005, r_{eD} = 500 s = 0), after Arad (2003)

The intersection between the unit-slope and the radial flow lines, Figure 5, provides *Equation 55:*

$$t_{D_{us,i}} = \frac{\pi\, r_{eD}^{\ 2}}{13{,}58} \tag{55}$$

A new expression to obtain the drainage area will result after replacing the respective dimensionless quantities, *Equation 56:*

$$r_e = \sqrt{\frac{k_f t_{us,i}}{877{,}3(\phi c)_{f+m}\,\mu}} \tag{56}$$

Combination of *Equation 51* and *56* will give,

$$\omega = 1{,}329\left(\frac{t_{pss}}{t_{us,i}}\right) \tag{57}$$

The dimensionless reciprocal rate curve presents a horizontal or constant behavior during the matrix-fracture transition period, Figure 5, which allows to obtain λ, *Equation 58:*

$$\lambda = \left\{\frac{1}{2}r_{eD}^2\left[(1/q_D)_{\text{inf}} - 1\text{n}(r_{eD}) + 0{,}75\right]\right\}^{-1} \tag{58}$$

As before, the following equality is found after replacing the dimensionless expressions, *Equation 59:*

$$\lambda = \left[\frac{r_e^2}{2(r_w e^{-s})^2}\left\{\left(\frac{k_f h\Delta m(P)(1/q)_{inf}}{141{,}2\,\mu B}\right) - \ln\left(\frac{r_e}{r_w e^{-s}}\right) + 0{,}75\right\}\right]^{-1} \tag{59}$$

The intersection of the unit-slope line during the transition period and the characteristic horizontal line of the reciprocal rate curve, also during the transition period, provides an expression which leads to calculate λ, see Figure 5:

$$\lambda = \left[\frac{1}{2}r_{eD}^2\left(\frac{6{,}79}{\pi\, r_{eD}^2}t_{D_{us,h}} - \ln(r_{eD}) + 0{,}75\right)\right]^{-1} \tag{60}$$

After plugging the dimensionless quantities, as before, yields in *Equation 61:*

$$\lambda = \frac{r_e^2}{2(r_w e^{-s})^2}\left(\frac{177{,}9\times 10^{-5} k_f}{\pi\,(\phi c_t)_t\,\mu\, r_e^2}t_{us,h} - \ln\left(\frac{r_e}{r_w e^{-s}}\right) + 0{,}75\right)^{-1} \tag{61}$$

An especial feature of the reciprocal rate curve is that it intercepts with the reciprocal rate derivative providing the following governing *Equation 62:*

$$t_{D_{rdi}} = \frac{1}{2}\omega r_{eD}{}^2\left[\ln(r_{eD}) - 0{,}75\right] \tag{62}$$

Suffix *"rdi"* stands for the intersection of the reciprocal rate curve and the reciprocal rate curve derivative. Combining this with *Equation 50* will yield in *Equation 63:*

$$r_{eD} = \exp\left(\frac{0{,}348 t_{rdi}}{t_{pss}} + 0{,}75\right) \tag{63}$$

Also, combination of *Equations 55* and *62* will result in *Equation 64:*

$$\omega = \frac{2{,}161}{(\ln(r_{eD}) - 0{,}75)}\frac{t_{rdi}}{t_{us,i}} \tag{64}$$

TOTAL SKIN FACTOR

The apparent skin factor is defined by *Equation 65:*

$$s' = s_t + Dq_{sc} \tag{65}$$

Many flow rates take place for the constant bottomhole pressure case. Then, assuming steady-state Darcy's flow applies *Equation 66:*

$$q_{sc} = \frac{0{,}703kh}{T}\frac{\Delta m(P)}{\ln(r_e/r_w)} \tag{66}$$

Then, using *Equation 66*, *Equation 65* can be written as:

$$s' = s_t + \frac{0{,}703khD}{T}\frac{\Delta m(P)}{\ln(r_e/r_w)} \tag{67}$$

It is suggested to run two well tests at different bottomhole pressure values so a procedure similar to the one outlined by Nuñez-Garcia, Tiab and Escobar (2003) can be applied for obtaining the total skin factor. Then *Equation 68.a*,

$$s_1' = s_t + \frac{0{,}703khD}{T}\frac{\Delta m(P)_1}{\ln(r_e/r_w)} \tag{68.a}$$

$$s_2' = s_t + \frac{0{,}703khD}{T}\frac{\Delta m(P)_2}{\ln(r_e/r_w)} \tag{68.b}$$

The simultaneous solution of *Equations 68.a* and *68.b* leads to obtain D and S_t values,

$$D = \frac{T\ln(r_e/r_w)}{0{,}703kh}\left(\frac{s_1' - s_2'}{\Delta m(P)_2 - \Delta m(P)_1}\right) \tag{69.a}$$

$$s_t = \frac{\Delta m(P)_2 s_1 - \Delta m(P)_1 s_2}{\Delta m(P)_2 - \Delta m(P)_1} \tag{69.b}$$

EXAMPLES

Example 1

The reciprocal rate and reciprocal rate derivative for a simulated well test of a naturally fractured reservoir with the transition period taking place during the late pseudosteady-state flow is shown in Figure 6. The input data for the simulation is given in Table 1. Find reservoir permeability, skin factor, drainage radius, interporosity flow parameter and dimensionless storativity coefficient for this problem.

Table 1. Reservoir, fluid and well data for examples

Parameter	Example 1	Example 2	Example 3
$\Delta m(P)$, psi^2/cp	68296876,83	30976300	16624499
ΔP, psi	500	580	350
h, ft	100	80	50
ϕ, %	20	25	5
r_w, ft	0,5	0,3	0,5
s	0	0	0
r_e, ft	500	30	1500
k, md	20	25	5
T, °R	710	670	610
γ_g	1,4	0,85	1,32
μg, cp	0,014	0,0122	0,0094
c_t, psi^{-1}	0,0019	0,0187	0,0036
ω	0,01	-	0,01
λ	1x10^{-6}	-	1x10^{-5}

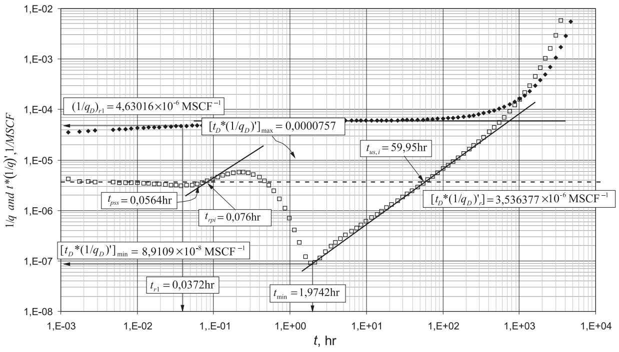

Figure 6. Reciprocal rate and reciprocal rate derivative for example 1 – heterogeneous reservoir with transition period during the late pseudosteady state

Solution

The following characteristic points are read from Figure 6.

$[t*(1/q)']_r = 3{,}536377\text{x}10^{-6}$ D/Mscf

$[t*(1/q)']_{min} = 8{,}9109\text{x}10^{-8}$ D/Mscf

$(1/q)r1 = 4{,}63016\text{x}10^{-6}$/Mscf

$t_{us,i} = 59{,}95$ hr

$t_{min} = 1{,}9742$ hr

$t_{pss} = 5{,}64\text{x}10^{-2}$ hr

$t_{rpi} = 7{,}6\text{x}10^{-2}$ hr

$t_{r1} = 3{,}72\text{x}10^{-2}$ hr

Permeability and apparent skin factor are obtained from *Equations 37* and *41.a*, respectively,

$$k_f = \frac{711{,}2664T}{h\Delta m(P)\left[t\times\left(1/q\right)'\right]_r} = \frac{711{,}2664(710)}{(100)(68296876{,}83)(3{,}536377\times10)^{-6}}$$

$= 20{,}9$ md

$$s = 0{,}5\left\{\left[\frac{\left(1/q_D\right)}{t\times\left(1/q\right)'}\right]_{r1} - \ln\left(\frac{k_2 t_{r1}}{(\phi c)_{1+2}\,\mu\, r_w^2}\frac{1}{\omega}\right) + 7{,}43\right\}$$

$$s=0,5\left\{\frac{\left(4,63016\times10^{-6}\right)}{\left(3,536377\times10^{-6}\right)}-\ln\left(\frac{(20)(0,0372)}{(0,2)\left(0,0019\right)(0,014)\,(0,5)^{2}}\frac{1}{(0,001)}\right)\right.$$

$$\left.+7,43\right\}=-5,7$$

The dimensionless storativity coefficient and interporosity flow parameter are respectively estimated from *Equation 43* and *47*.

$$\omega=0,15866\frac{\left[t_D\times\ (1/q_D)'\right]_{\min}}{\left[t_D\times\left(1/q_D\right)'\right]_r}+0,54653\left\{\frac{\left[t_D\times\left(1/q_D\right)'\right]_{\min}}{\left[t_D\times\ (1/q_D)'\right]_r}\right\}^2$$

$$\omega=0,15866\frac{(8,9109\times10^{-8})}{(3,536377\times10^{-6})}+0,54653\left[\frac{(8,9109\times10^{-8})}{(3,536377\times10^{-6})}\right]^2=0,0043$$

$$\lambda=\frac{(\phi c)_{f+m}\,\mu\, r_w^2}{0,0002637k_f\,t_{us,i}}=\frac{(0,2)\left(0,0019\right)(0,014)\,(0,5)^2}{0,0002637(20)(59,95)}=4,2\times10^{-6}$$

Again, the dimensionless storativity coefficient is estimated using *Equation 57*, thus:

$$\omega=1,329\left(\frac{t_{pss}}{t_{us,i}}\right)=1,329\left(\frac{5,64\times10^{-2}}{59,95}\right)=1,25\times10^{-3}$$

The drainage radius is estimated with *Equation 56,*

$$r_e=\sqrt{\frac{k_f\,t_{us,i}}{877,3\left(\phi c\right)_{f+m}\mu}}=\sqrt{\frac{(20)(59,95)}{877,3\left(0,2\right)(0,0019)(0,014)}}=506,85\text{ft}$$

Once again, the dimensionless storativity coefficient is recalculated with *Equation 51*, thus:

$$\omega=\frac{4,7599\times10^{-3}k_f\,t_{pss}}{\pi r_e^{\,2}\left(\phi c\right)_t\,\mu}=\frac{4,7599\times10^{-3}(20)(5,64\times10^{-2})}{\pi\,(506,85)^2\left(0,2\right)(0,0019)(0,014)}=2,5\times10^{-3}$$

Example 2

Figure 7 presents the reciprocal rate and reciprocal rate derivative for a simulated well test of a homogeneous bounded reservoir. As for example 1, the data used for the simulation is given in Table 1. Find reservoir permeability, skin factor and drainage radius for this example.

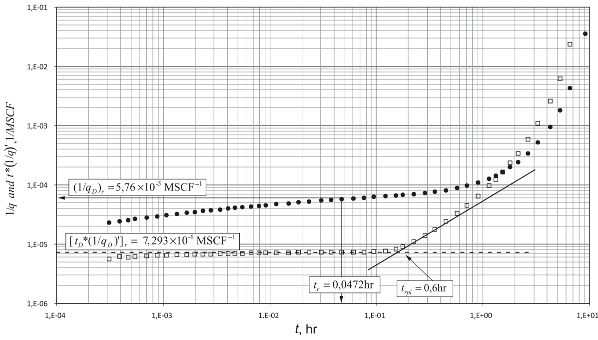

Figure 7. Reciprocal rate and reciprocal rate derivative for example 2 – homogeneous reservoir

Solution

The following information is read from Figure 7:

$[t*(1/q)']r$ = 7,293x10^{-6} D/Mscf

$(1/q)r$ = 5,76x10^{-5} D/Mscf

t_{pss} = 5,64x10^{-2} hr

t_{rpi} = 0,06 hr

t_r = 4,72x10^{-2} hr

Equations. 13, *25* and *30*, are used to obtain permeability, skin factor and drainage.

$$k=\frac{711,5817T}{h\Delta m(P)\left[t\times\left(1/q\right)'\right]_r}=\frac{711,5817(670)}{(80)(30976300)(7,293\times10)^{-6}}=26,37\text{ md}$$

$$s'=0,5\left\{\frac{\left(5,76\times10^{-5}\right)}{(7,293\times10^{-6})}-\ln\left(\frac{(25)(0,0472)}{(0,25)\,(0,0122)(0,00187)(0,3)^2}\right)+7,43\right\}=0,68$$

$$r_e=22,727\times10^{-3}(0,3)\left(\frac{(25)}{(0,25)(0,0122)(0,00187)(0,3)^2}\right)^{0,4627}(0,6)^{0,4627}=19,5$$

Example 3

The reciprocal rate and reciprocal rate derivative for a simulated well test for a naturally fractured reservoir with the transition period taking place during the radial flow regime is shown in Figure 8. The input data for the simulation is also given in Table 1. For this example find reservoir permeability, skin factor, drainage radius, interporosity flow parameter and dimensionless storativity coefficient.

Solution

The following characteristic points are read from Figure 6.

$[t*(1/q)']_r$ = 0,000107 D/Mscf

$[t*(1/q)']_{min}$ = 5,45x10^{-6} D/Mscf

$(1/q)_{r2}$ = 0,00151/Mscf

$t_{us,i}$ = 43 hr

t_{min} = 1,46 hr

t_{rpi} = 600 hr

t_{r2} = 187,123 hr

Permeability and apparent skin factor are obtained from *Equations 37* and *41.b*, respectively,

$$k_f = \frac{711{,}2664T}{h\Delta m(P)\left[t\times(1/q)'\right]_{r1,r2}} = \frac{711{,}2664(610)}{(50)(16624499)(0{,}000107)} = 4{,}9 \text{ md}$$

$$s' = 0{,}5\left\{\frac{(0{,}0015)}{(0{,}000107} - \ln\left[\frac{(5)(187{,}123)}{(0{,}05)(0{,}0036)\,(0{,}094)(0{,}5)^2}\right] + 7{,}43\right\} = 1{,}1$$

The naturally fractured reservoir parameters are estimated with *Equations 43* and *47*,

$$\omega = 0{,}15866\frac{(5{,}45\times10^{-6})}{(0{,}000107)} + 0{,}54653\left[\frac{(5{,}45\times10^{-6})}{(0{,}000107)}\right]^2 = 0{,}009$$

$$\lambda = \frac{(\phi c)_{f+m}\,\mu r_w^2}{0{,}0002637k_f\,t_{us,i}} = \frac{(0{,}05)(0{,}0036)(0{,}094)(0{,}5)^2}{0{,}0002637(5)(43)} = 7{,}5\times10^{-5}$$

ANALYSIS OF RESULTS

From the simulated examples is observed that the estimated parameters are in good agreement with the input values, except for the apparent skin factor which presents some variations from simulated runs in fractured wells and naturally fractured reservoirs. However, based upon the good results, there is implied that the TDS technique works accurately and practically. For space saving purposes not all the equations were reported in the worked examples. However, they also present a good degree of accuracy and may be applied by the reader in his/her own field of practice. Finally, the differences between the simulated and estimated skin factors may be due to turbulence effects.

CONCLUSIONS

- For multiphase flow, new equations are introduced to the TDS technique for estimation of phase permeabilities, wellbore storage coefficient, skin factor and reservoir drainage area. The application of the equations was verified through field and simulated well test data.

- A new set of equations for interpretation of well test data from constant bottomhole pressure is presented following the philosophy of the TDS technique. These equations were proved to work accurately with synthetic test data.

- The results provided in this article show that well test analysis methods for wells produced at constant pressure provide the same information about the reservoir as is determined from the conventional methods for the constant-rate production case. Therefore, the transient rate data analysis may be used as an alternative method in the absence of the transient pressure data.

- Unlike the typical decline-type curves presented by Fetkovich, the results obtained by the TDS technique are verifiable. The solutions provided here reveal that the various sorts of reservoir heterogeneities affect the rate behavior which is reflected when having the transition period during the late pseudosteady state period and, due to due to the rate exponential behavior, the reciprocal rate and pressure solutions are very different for boundary dominated flow period. Therefore, the decline-type curves may not be able to capture these details and may lead to unreliable results.

ACKNOWLEDGMENTS

The authors gratefully acknowledge the financial support of both Ecopetrol S.A.-Instituto Colombiano del Petróleo (ICP) and Universidad Surcolombiana, Neiva, Huila.

REFERENCES

Arab, N. (2003). Application of Tiab's Direct Synthesis Technique to Constant Bottom Hole Pressure Tests. *M. S. Thesis*, The University of Oklahoma, USA.

DaPrat, G., Cinco-Ley, H., & Ramey, H. J. Jr. (1981). Decline Curve Analysis Using Type Curves for Two-Porosity System, June. *SPEJ* 354-62.

Engler, T. and Tiab, D., (1996). Analysis of Pressure and Pressure Derivative Without Type Curve Matching, 4. for Naturally Fractured Reservoirs. *J. Petroleum Scien. and Engineer.*, 15:127-138.

Fetkovich, M. J. (1980). Decline Curve Analysis Using Type Curves. *J. Petroleum Technol.*, June, 1065-1077.

Nuñez-García, W., Tiab, D., & Escobar, F. H. (2003). Transient Pressure Analysis for a Vertical Gas Well Intersected by a Finite-Conductivity Fracture. *SPE Production and Operations Symposium*, Oklahoma City, OK, U.S.A., March 23–25. SPE 15229.

Tiab, D. (1995). Analysis of Pressure and Pressure Derivative without Type-Curve Matching: 1- Skin Factor and Wellbore Storage. *J. Petroleum Scien. and Engineer.*, 12: 171-181.

Tiab, D. & Escobar, F. H. (2003). Determinación del Parámetro de Flujo Interporoso a Partir de un Gráfico Semilogarítmico. *X Congreso Colombiano del Petróleo.*, Bogotá, Colombia, Oct. 14-17.

Van Everdingen, A. F., & Hurst, W. (1949). The Application of the Laplace Transformation to Flow Problems in Reservoirs. *Trans. AIME (Amer. Inst. Min. Metall. Eng.),* 186: 305-320.

Vongvuthipornchai, S., & Raghavan, R. (1988). A Note on the Duration of the Transitional Period of Responses Influenced by Wellbore Storage and Skin. *SPE Formation Evaluation*, 207-214.

Warren, J. E. & Root, P. J. (1963). The Behavior of Naturally Fractured Reservoir. *Soc. Pet. Eng. Journal.* Sept., 245-255.